Supporting Information for "Atomistic Study of Dynamic Contact Angles in CO_2-Water-Silica System"

Pengyu Huang [a], Luming Shen [a,*], Yixiang Gan [a], Federico Maggi [a], Abbas El-Zein [a], and Zhejun Pan [b]

[a] School of Civil Engineering, Building J05, The University of Sydney, NSW 2006, Australia

[b] CSIRO Energy, Private Bag 10, Clayton South, VIC 3169, Australia

*Corresponding author. Email: luming.shen@sydney.edu.au; Tel: +61-2-93512126; Fax: +61-2-93513343.

Number of pages: 13, Number of figures: 4, Number of tables: 2

The Supporting Information document includes the following sections:

S1. Surface structure of the Q^3 silica surface

S2. Force field equations and parameters

S3. Water droplet on silica substrate

S4. Contact angle calculation

S5. Calculations of the cumulative percentage curve

S6. Calculation of interfacial tension between CO_2 and water

References

S1 Surface structure of the Q^3 silica surface

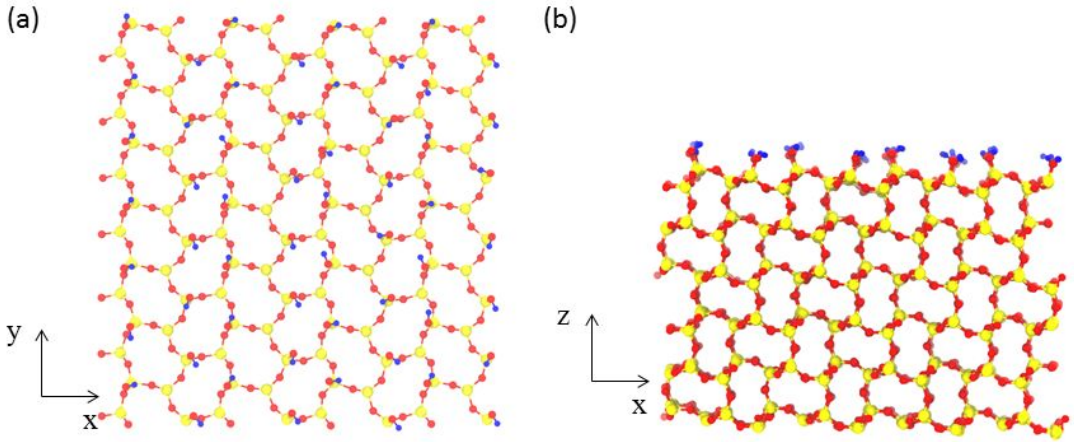

Figure S1. (a) Top view and (b) side view of the Q^3 silica surface[1] used in our model. The oxygen atoms are in red, the silicon atoms in yellow, and the hydrogen atoms in blue. The images are plotted using the visualization tool for molecular dynamics VMD.[2]

S2 Force field equations and parameters

The selected molecular models use Lennard-Jones (LJ) potential and coulombic interactions for modelling the intermolecular interactions. The pair potential u_{ij} between the i-th and j-th atoms, separated by a distance r_{ij} is calculated as:

$$u_{ij} = 4\varepsilon_{ij}\left[\left(\frac{\sigma_{ij}}{r_{ij}}\right)^{12} - \left(\frac{\sigma_{ij}}{r_{ij}}\right)^{6}\right] + \frac{q_i q_j}{4\pi\varepsilon_o r_{ij}^2}, \quad \text{(S1)}$$

where ε_{sl} and σ_{sl} are the depth and distance of the potential well for the LJ potential term, and ε_o is the vacuum permittivity, q_i and q_j are the charges on the i-th and j-th atoms. Table S1 lists the parameters for the molecular models used in this work. The first term in Eq. (S1) is the Lennard-Jones potential function, and a cut-off radius of 1.2 nm is chosen for all cases. For the interactions between unlike atoms, the Lorentz Berthelot mixing rule is used, as in Ref. [1]. The last term in Eq. (S1) is the coulombic interaction, and it is calculated using the particle-particle particle-mesh method[3] with a relative error in forces of 10^{-5}. The intramolecular interactions are described by harmonic bond and harmonic angle equations except for the water molecules. The potential energy for bond E_{bond} and angle E_{angle} are calculated as:

$$E_{bond} = K_{bond}(r - r_o)^2 \quad \text{(S2)}$$

$$E_{angle} = K_{angle}(\theta - \theta_o)^2, \quad \text{(S3)}$$

where the K_{bond} and K_{angle} are the stiffness parameters for bond and angle interactions, respectively; r_o and θ_o are the equilibrium bond length and angle for the molecules,

respectively; r is the instantaneous distance between two bonded atoms, and θ is the instantaneous angle for the relevant atoms. Table S2 reports the values of the parameters used in the bond and angle equations.

Table S1. The parameters of Lennard Jones and columbic interactions

Molecule model	Atom	ε(kcal/mol)	σ (Å)	Charge (e)	OM distance(Å)
CO_2 (EMP2) [4]	C	0.0559	2.757	0.6512	-
	O_c	0.1597	3.033	-0.3256	-
H2O (TIP4P/2005) [5]	H_w	0	0	0.5564	-
	O_w	0.1852	3.1589	-1.1128	0.1546
Silica[1]	Si	0.093	3.6972	1.1	-
	O(bulk)	0.054	3.0914	-0.55	-
	O(silanol)	0.122	3.0914	-0.675	-
	H(silanol)	0.015	0.9666	0.4	-

Table S2. The values of the parameters for the bond and angle interactions

Molecule	Bond	K_{bond} (kcal/(mol·Å^2))	r_o (Å)	Angle	K_{angle} (kcal/(mol·rad^2))	θ_o (°)
CO_2[4]	C-O_c	1283.38	1.149	O_c -C-O_c	147.7	180
H2O[5]	H_w-O_w	-	0.9572	H_w-O_w-H_w	-	104.52
Silica[1]	H-O	495	0.945	H-O-Si	50	115
	O-Si	285	1.68	O-SI-O	100	109.5
				Si-O-Si	100	149

S3 Water droplet on silica substrate

We performed a simple test for modelling a water droplet on the Q^3 silica surface with a rigid tip4p/2005 water model at 333.15 K. SHAKE algorithm was used to apply the bond and angle constraints onto the rigid water molecules. Initially, a half sphere droplet of water (1737 molecules) with a radius of 3 nm was placed on the top of a silica slab, in a periodic simulation box with a size of 22.4×24.4×8 nm^3. The snapshot of the system at the beginning of the simulation is shown in Figure S2 (a). The water droplet was obtained from an equilibrated water box at T = 333.15 K and the atmospheric pressure. The system was run initially using the Langevin thermostat algorithm[6] for the system to reach thermal equilibrium quickly for the first 1 ns. Then, the system was run with the Nosé-Hoover chains thermostat[7] for the rest of the simulation until it was equilibrated. The system was found to be in equilibrium at around 6 ns. The snapshot of the system at the equilibrium state is shown in Figure S2 (b). A contact angle of zero was observed, as indicated by the snapshot. It was also found that the contact angle for the water droplet on the Q^3 silica surface should be zero, as indicated in the MD simulations for the Q^3 silica surface[1] (with flexible SPC water model) and in the experiments for fully hydroxylated quartz surfaces.[8]

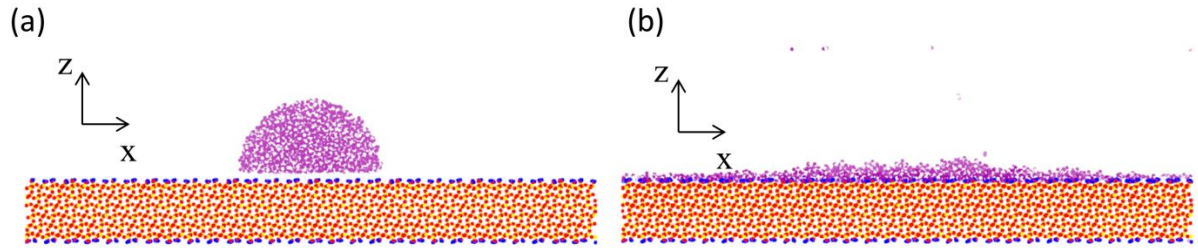

Figure S2 – Snapshots of the system for modeling a droplet on the silica substrate at: (a) the initial state, and (b) the equilibrium state. The images are plotted using the visualization tool for molecular dynamics VMD.[2]

S4 Contact angle calculation

During the MD simulations, the 2D water density profile was obtained based on the coordinates of atoms. Firstly, the simulation box was divided into small bins (square columns) with a width of 0.2 nm in the x-direction and a height of 0.2 nm in the z-direction. Then, the time-averaged density was calculated in each bin every 1 ns to obtain the 2D density profile. As the CO_2-water interface moves in the dynamic contact angle simulations, the interface estimated from the time-averaged density over every Δt = 1 ns may not be very accurate, especially at a high flow velocity. Therefore, for the simulations with the piston moving at greater than or equal to 1 m/s, the time-averaged density was obtained at every 0.01 ns by averaging the coordinates of the atoms in each bin. If the piston has moved one bin width forward (0.2 nm) in the x-direction, the 2D density profile is shifted one bin width back in the x-direction accordingly. Since the periodic boundary condition in the x-axis was applied, if the x-coordinates of the bins were smaller than 0 after the shift, it would be added back to the other end in the x-axis. Now we can calculate the average of 100 samples of these 2D density profiles to obtain the time-average density profile every Δt for the dynamic case.

After the 2D water density profile had been obtained, the curved interface was determined from the density contour at the location with a half of the bulk water density. Figure 3(a) shows how the contact angle was measured by fitting the data with a 2nd order polynomial function to calculate the bottom and top contact angles. The contact angles were calculated as the angles between the fitted polynomial functions and the horizontal lines which represent the silica surfaces, as shown in Figure 3(a). As the water density close to the silica surface varies significantly (Figure 3(b)), due to strong interactions between water molecules and the solid surface and the poor samplings near the surface, only the interface data that was 0.8 nm away from the solid surface was used to fit the polynomial function. In order to have the 2nd

order polynomial function to fit the interface data more precisely, the coordinates of the interface data that were within 1 nm to the centre of the channel height were not used for the fitting either. During the production run, the contact angles were calculated at every 1 ns from the 2D water density contour. The average and the standard deviations of the contact angles were then calculated.

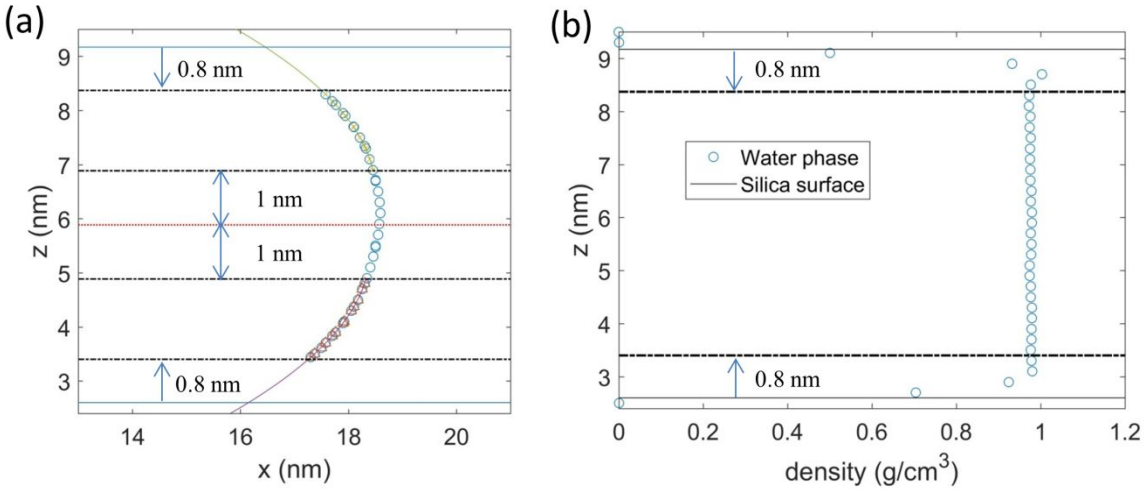

Figure S3. (a) An example of contact angle measurement. The data plotted with triangle and cross markers are used to fit the 2nd order polynomial function for the bottom and top parts, respectively. The light blue solid lines represent the position of the silica surfaces. The red dotted line is the middle of the channel height. (b) Density changes along the z-axis in the bulk water region. The gray solid lines represent the positions of the silica surfaces.

S5 Calculations of the cumulative percentage curve

The equilibrium jump frequency in the parallel and perpendicular directions $K_{o,\parallel}$ and $K_{o,\perp}$ were calculated using the coordinates of molecules obtained from the equilibrium simulations. Theoretically, the trajectories of the molecules in the three-phase contact line zone should be analysed. However, the three-phase contact line zone is subject to the large fluctuations due to the small number of molecules involved in the interface. Therefore, the analysis was done for the bulk water and CO_2 regions in the first layers for the static case after equilibrium, by assuming that the behaviours of the molecules at the three-phase contact line would be similar. Since both the top and bottom silica surfaces were the same, only the molecules on the bottom layer were investigated. To calculate $K_{o,\parallel}$ and $K_{o,\perp}$, we first counted the molecules of one fluid (water or CO_2) on the first layer in the bulk region once the system was equilibrated (after 5 ns). The distance for each molecule had travelled from its initial position was then calculated every 1 ps. If the travelled distance of one molecule was greater than the parallel jump distance $\lambda_{\parallel}$ in the x or y directions, then we considered a parallel jump had occurred. Similar, if one molecule had travelled a distance greater than the perpendicular jump distance $\lambda_{\perp}$, one perpendicular jump was counted. The cumulative counting lasted until most of the molecules had left from the first liquid layer near the surface. The cumulative percentage of molecules which had made a parallel jump or a perpendicular jump in the first layer was calculated as a function of time. Multiple cumulative percentage curves were obtained by repeating the counting process until the end of the simulations. In the end, the average cumulative percentage curve can be plotted and used to calculate $K_{o,\parallel}$ and $K_{o,\perp}$, as shown in the manuscript. The method of block average was used to estimate the errors of $K_{o,\parallel}$ and $K_{o,\perp}$.[9] The cumulative percentage curves were divided into 10 blocks. At each block, the cumulative percentage curves were averaged, and $K_{o,\parallel}$ and $K_{o,\perp}$ were calculated from the

144 averaged cumulative percentages curve. Then, the standard deviations of the $K_{o,\parallel}$ and $K_{o,\perp}$

145 obtained from the 10 blocks were calculated as the estimated errors of $K_{o,\parallel}$ and $K_{o,\perp}$.

146

S6 Calculation of interfacial tension between CO_2 and water

S6.1 Method

To calculate the interfacial tension of the CO_2-water system at a specific temperature T, the CO_2-water interface simulation was performed. At first, a simulation box of L_x = 20 nm and $L_y = L_z$ = 5 nm was created and the periodic boundary conditions were applied in all three directions. Water molecules were generated randomly in the middle of the simulation box (-4.9 nm < x <4.9 nm) and two groups of CO_2 molecules were also generated and placed at the two sides of the water molecules (-9.9 nm < x < -5.1 nm and 5.1 nm < x < 9.9 nm). After the generation of the molecules, energy minimization was performed to avoid the large stresses induced by the overlaps between molecules. Three different simulation boxes were created with the same number of water molecules: 8,287 molecules, but different numbers of CO_2 molecules N_{co2}: (1) N_{co2} = 336; (2) N_{co2} = 848 and (3) N_{co2} = 2,476. These three values of N_{co2} were estimated from the equation of state of the CO_2 under three different pressures: P = 5, 10 and 20 MPa. For the molecular dynamics simulation, the system was initially run under the Langevin thermostat[6, 10] (under the constant number of molecules, constant volume and constant temperature ensemble, i.e. *NVT* ensemble) for the purpose of the quick relaxation and equipartitioning of kinetic energy for 0.1 ns. Afterward, the system was further equilibrated under the constant-number of molecules, constant temperature and constant pressure along the x-axis, i.e. NP_xT ensemble for another 1 ns. The NP_xT ensemble simulation was achieved by using both Nosé-Hoover chains thermostat and a Parrinello-Rahman barostat.[7, 9, 11, 12] A temperature of 333.15 K was used, but six targeted normal pressures were considered in the simulations: P_{xx} = 3, 5, 10, 15, 20, and 25 MPa. The system created with N_{co2} = 336 was used for P_{xx} = 3 and 5 MPa; the system created with N_{co2} = 848 was used for P_{xx} = 10 MPa; and the system created with N_{co2} = 2,476 was used for P_{xx} = 15, 20, and 25 MPa. After the equilibration under the NP_xT ensemble, the simulations were switched to *NVT*

ensemble using a Nosé-Hoover chains thermostat and ran for 4.4 ns. The interfacial tension was calculated from the data obtained from the last 2.4 ns of the simulation. The time step of 1 fs (10^{-15} s) was used. The force fields and molecular models were same as those used in the contact angle simulations. The damping parameters of the temperature and pressure were set to be 100 fs and 1000 fs, respectively, when applicable. The interfacial tension γ was calculated using the following equation:[13]

$$\gamma = \frac{1}{2} L_x < P_{xx} - \frac{P_{yy} + P_{zz}}{2} > , \quad \text{(S4)}$$

where P_{xx}, P_{yy}, and P_{zz} are the virial pressure components and L_x is the length of the box in the x-direction. The instantaneous value of γ was calculated at every 50 fs. The statistical errors of the surface tension were estimated by calculating the statistical inefficiency.[9, 14, 15]

For comparison, the interfacial tension between CO_2-water was estimated from the static contact angle simulations from the Young-Laplace equation:

$$\gamma = \frac{\Delta P_s h}{2 cos\theta_w} \quad \text{(S5)}$$

where ΔP_s is the difference between bulk CO_2 pressure and bulk water pressure, h is the height of the channel, and θ_w is the static contact angle of the water phase.

S6.2 Results

Figure S4 shows the interfacial tension computed from the results of the static contact angle simulations (Eq. (S5)) and from the CO_2-water interface simulations (Eq. (S4)). The experimental data[16] is also plotted in Figure S4 for comparison. It should be noted that the experimental data was obtained at 333.5 K instead of 333.15 K. We can see that the interfacial tensions calculated from the CO_2-water interface simulations match well with the experimental data for CO_2 pressure P_{co2} < 10 MPa, while for Pco_2 > 10 MPa the simulated

interfacial tension values are overestimated by around 15~30%. The values of interfacial tension calculated from the static contact angle simulations and Eq. (S5) were larger than those calculated from the CO_2-water interface simulations as well as the experimental data. One possible reason for this discrepancy could be the Young-Laplace equation may not hold at the nano-scale, which may be caused by the differences between the pressures on CO_2-silica and water-silica interfaces and the bulk CO_2 and water pressures. However, detailed studies are required to draw such a conclusion. Despite the difference at the high pressure, a similar trend was observed for all three cases, namely, the interfacial tension values decreased more rapidly for P_{co2} from 0 to around 10 MPa, while the effect of the CO_2 pressure (or normal pressure for the CO_2-water interface simulation) on interfacial tension was much less significant for Pco_2 > ~ 10 MPa. This can be attributed to the fact that the density of the CO_2 changes significantly for P_{co2} increasing from 0 to around 13 MPa,[17] affecting the interfacial properties. For the dynamic contact angle simulations, the calculated P_{co2} was around 20 MPa, therefore, γ = 0.035 N/m was used in the molecular kinetic theory (MKT) equations and the calculation of the capillary number *Ca* in this work, as reported in the manuscript.

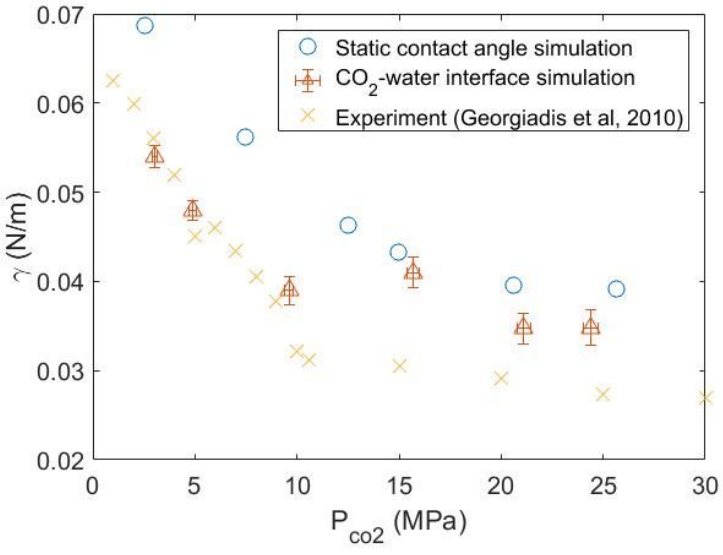

Figure S4. The interfacial tensions are plotted as a function of the bulk CO_2 pressure. The pressure in the normal direction to the CO2-water interface simulations was assumed to be the bulk CO_2 pressure, as the normal pressure should be statistically constant in both CO_2 and water phases.

References

1. Emami, F. S.; Puddu, V.; Berry, R. J.; Varshney, V.; Patwardhan, S. V.; Perry, C. C.; Heinz, H., Force field and a surface model database for silica to simulate interfacial properties in atomic resolution. *Chem. Mater.* **2014,** *26* (8), 2647-2658.
2. Humphrey, W.; Dalke, A.; Schulten, K., VMD: visual molecular dynamics. *Journal of molecular graphics* **1996,** *14* (1), 33-38.
3. Hockney, R. W.; Eastwood, J. W. *Computer simulation using particles*. crc Press: 1988.
4. Nieto-Draghi, C.; de Bruin, T.; Pérez-Pellitero, J.; Bonet Avalos, J.; Mackie, A. D., Thermodynamic and transport properties of carbon dioxide from molecular simulation. *J. Chem. Phys.* **2007,** *126* (6), 064509.
5. Abascal, J. L.; Vega, C., A general purpose model for the condensed phases of water: TIP4P/2005. *J. Chem. Phys.* **2005,** *123* (23), 234505.
6. Schneider, T.; Stoll, E., Molecular-dynamics study of a three-dimensional one-component model for distortive phase transitions. *Phys. Rev. B* **1978,** *17* (3), 1302.
7. Shinoda, W.; Shiga, M.; Mikami, M., Rapid estimation of elastic constants by molecular dynamics simulation under constant stress. *Phys. Rev. B* **2004,** *69* (13), 134103.
8. Lamb, R. N.; Furlong, D. N., Controlled wettability of quartz surfaces. *Journal of the Chemical Society, Faraday Transactions 1: Physical Chemistry in Condensed Phases* **1982,** *78* (1), 61-73.

9. Allen, M. P.; Tildesley, D. J. *Computer Simulation of Liquids*. Oxford University Press: New York, 1987.

10. Dünweg, B.; Paul, W., Brownian dynamics simulations without Gaussian random numbers. *International Journal of Modern Physics C* **1991,** *2* (03), 817-827.

11. Frenkel, D.; Smit, B. *Understanding Molecular Simulation: From Algorithms to Applications*. Academic Press: San Diego, 2001; Vol. 1.

12. Martyna, G. J.; Tobias, D. J.; Klein, M. L., Constant pressure molecular dynamics algorithms. *J. Chem. Phys.* **1994,** *101* (5), 4177-4189.

13. Ismail, A. E.; Grest, G. S.; Stevens, M. J., Capillary waves at the liquid-vapor interface and the surface tension of water. *J. Chem. Phys.* **2006,** *125* (1), 014702.

14. Friedberg, R.; Cameron, J. E., Test of the Monte Carlo method: fast simulation of a small Ising lattice. *J. Chem. Phys.* **1970,** *52* (12), 6049-6058.

15. Fincham, D.; Quirke, N.; Tildesley, D., Computer simulation of molecular liquid mixtures. I. A diatomic Lennard-Jones model mixture for CO2/C2H6. *J. Chem. Phys.* **1986,** *84* (8), 4535-4546.

16. Georgiadis, A.; Maitland, G.; Trusler, J. M.; Bismarck, A., Interfacial tension measurements of the (H2O+ CO2) system at elevated pressures and temperatures. *Journal of Chemical & Engineering Data* **2010,** *55* (10), 4168-4175.

17. Iglauer, S.; Mathew, M.; Bresme, F., Molecular dynamics computations of brine–CO2 interfacial tensions and brine–CO2–quartz contact angles and their effects on structural and residual trapping mechanisms in carbon geo-sequestration. *J. Colloid Interface Sci.* **2012,** *386* (1), 405-414.